Re-examination of Color-Flavor Unlocking in Strange Quark Matter — Continuous Phase Transition or Asymptotic Smooth Unlocking? —

Hiroaki Abuki
Yukawa Institute for Theoretical Physics, Kyoto University, Kyoto, Japan
(Dated: January 27, 2020)

We revisit the unlocking transition from the color-flavor locked (CFL) phase to the two-flavor pairing (2SC) phase paying a special attention to the multiplicity of the gap parameters. By deriving the exact expression of the effective potential for 5-gap parameters, we show that the CFL phase is much robuster against the increase of the strange quark mass than is predicted by the kinematical criterion for the unlocking. As temperature is decreased, the CFL phase gets stronger against the strange quark mass, and at zero temperature, even a possibility of surviving CFL pairs for all finite value of strange quark mass manifests itself. In this case, the 2SC phase may be realized as the asymptotic limit of the distorted CFL state as $M_s \to \infty$. The unlocking transition triggered by increasing strange quark mass is of continuous 2nd order rather than of 1st order at finite temperature. At zero temperature, we cannot conclude even an existence of unlocking for some numerical difficulties and also for the limit of the adopted model. But if it exists, it is most likely of weak 2nd order. We also find the fact that the color-flavor locking state actually corresponds to a saddle point of the effective potential, which is unstable in the three out of five directions. Physical interpretation for this fact is examined.

PACS numbers: 12.38.-t, 12.38.Aw, 25.75.Nq

I. INTRODUCTION

Since a possible color superconducting phase was proposed by Bailin and Love [1], the dynamics of QCD under high baryon density has been attracted much interests [2] and is revealing its rich and interesting phase structures [3]. In particular, the color-flavor locked (CFL) type of the pairing order [4] is most likely to emerge at sufficiently high quark chemical potential for relatively small strange quark mass M_s [5, 6, 7, 8, 9]. In contrast to this solid fact, however, the phases for larger and realistic value of M_s^2/μ are not uncovered yet, and so many phases have been proposed and various phase transitions have been studied so far: These include: the simple scenario of the unlocking transition from the CFL to the two-flavor ordering (2SC) state [10, 11], the inhomogeneous LOFF (Larkin-Ovchinnikov-Fulde-Ferrell) type of the pairing state [12, 13], the CFL state with kaon (K^0, K^+) condensation [14], the gapless 2SC state [15] and its CFL version [16], and dSC state [17], and which phase to be favored for realistic value of M_s remains a still controversial problem.

The unlocking transition from the CFL state to the 2SC state with increasing the value of M_s^2/μ is firstly investigated using Nambu–Jona-Lasinio (NJL) type effective models [10, 11]. Their results show that as the strange quark mass is increased, the 1st order unlocking transition takes place at some critical M_s^c, and a simple kinematical criterion for the critical mass works quite well. This criterion is based on the observation that the transition from the CFL to the 2SC with increasing M_s would occur when the mismatch of the Fermi momenta of light and strange quark becomes as large as the magnitude of the gap. In Ref. [10], the fermionic dispersions are approximately constructed by the expansion in the flavor breaking parameter M_s^2/μ, and after that, the effective potential is constructed from these dispersions. Inappropriate approximation often leads an appearance of wrong blocking region in the kernel of the gap equation, and this also maybe results in the wrong phase transition. On the other hand, in Ref. [11], the coupled gap equation is exactly solved with non-perturbative treatment of M_s. However, one must say that their construction of the effective potential is quite ambiguous and, as we shall show, maybe possibly fails because of the multiplicity of the gap parameter. Even though their results are in good accordance with each other, there still exist a possibility that they missed the true solution. Furthermore, we have no strong universality argument that the unlocking transition must be of 1st order one, because the $SU(3)_V$ is already fallen into the $SU(2)_V$ isospin symmetry in the presence of finite strange quark mass.

In the present paper, we study the unlocking transition in more complete way than has been taken in past work, by making a proper use of the Pauli construction of exact effective potential[1]. In particular, we study how the CFL state and other states are realized in the multi-gap parameter space and how the potential surface gets distorted

[1] This procedure generates a non-trivial quadratic mean field term in the effective potential. The author thanks T. Kunihiro for pointing its importance out.

with increasing the value of M_s^2/μ. Throughout this paper, we ignore the local neutrality conditions and treat the strange quark mass M_s as a parameter and draw phase diagrams in $(\mu; T; M_s)$ parameter space, leaving more complete self-consistent analyses in future problems.

This paper is organized as follows. In Sec. II, we introduce our model, and present a general framework to obtain the gap equation and the effective potential, taking special care of the multiplicity of the gap parameter. Sec. III is devoted to the numerical analyses on the gaps, effective potential varying the strange quark mass and temperature of the system. The phase structure in $(T; \mu; M_s)$ parameter space in our model is unveiled. In Sec. IV, we make summary and concluding remarks of this work.

II. FORMULATION

In this section, we present an outline for obtaining the gap equations and the effective potential with which we can determine the ground state of the system characterized by $(\mu; T; M_s)$ parameter. We give a framework to derive the gap equation, which is applicable even for the more general case with the non-local interaction than with point-like interaction, until we specify the detail of our model in Sec. IIB.

A. Gap equations

Gap equation can be constructed by the self-consistency condition for 1PI (proper) self-energy. We specify the model space by color, flavor and spinor structure of the self-energy. As for the spinor structure, we consider the case of $J^P = 0^+$ channel only, and which is guaranteed by γ_5 in the self-energy matrix.

Self energies. We first introduce the color-flavor mixed quark base: $q = \sum_{a,i} \frac{1}{\sqrt{2}} \lambda_a^i q_i^a$; where λ^a $(a = 1 \cdots 8)$ are the Gell-Mann matrices and we defined $(\lambda^9)_i^a = \sqrt{\frac{2}{3}}\,\delta_i^a$. Then the Nambu-Gor'kov propagator in the 2-component quark field $Q = (q; q^t)$ is written as

$$S(q_0; q) \equiv -i\langle T_\tau Q(x) \bar{Q}(0)\rangle = \begin{pmatrix} \not{q}_+ - M & \Delta(q_0; q) \\ \gamma_0 \Delta(q_0; q)^\dagger \gamma_0 & \not{q}_-^t - M^t \end{pmatrix}^{-1}. \tag{1}$$

$\Delta(q_0; q)$ is off-diagonal self-energy which gives rise to gaps in the quasi-quark dispersion. M is the quark mass matrix in the color-flavor mixed base:

$$M = \begin{pmatrix} 0 & 0_3 & \frac{M_s}{2}(1_2 + \tau_2) \\ 0_3 & 0 & \frac{M_s}{2}(1_2 + \tau_2) \\ \frac{2M_s}{3} & \frac{2M_s}{3} & \frac{M_s}{3} \end{pmatrix}. \tag{2}$$

Here, $\tau = (\tau_1; \tau_2; \tau_3)$ are the Pauli matrices. The pure CFL ansatz for the off-diagonal self-energy is expressed in the color-flavor mixed base as following,

$$\Delta^{\rm CFL}(q_0; q) = C\gamma_5 \Phi^{ab3} 1_8 \begin{pmatrix} 1 & & \\ & 1 & \\ & & 1 \end{pmatrix}. \tag{3}$$

Here, C is the charge conjugation matrix $C = i\tau_2\gamma_0$. On the other hand, we would have the 2SC state with u-d pairing $\Phi^{2SC_{ud}} = \epsilon_{ij} \Phi^{ab3}$ $\Phi^{2SC} = A_{ij} \Phi^{ab3}$ for sufficiently large value of M_s, which is written as

$$\Delta^{2SC_{ud}}(q_0; q) = C\gamma_5 \Phi^{2SC} \begin{pmatrix} 0 & 1_3 & \\ 0_4 & & \\ & & \end{pmatrix} \begin{pmatrix} & & \\ & & \\ \frac{1}{3} & \frac{\sqrt{2}}{3} & \\ \frac{\sqrt{2}}{3} & \frac{2}{3} & \end{pmatrix}; \tag{4}$$

in the color-flavor mixed base. As we shall derive later, the gap equation for this 2SC state does not depend on the value of M_s. From the two expressions for the 2SC and CFL phases, it is quite natural to expect the distorted CFL

state (dCFL), the minimal interpolating pairing ansatz between those phases, for the small but finite strange quark mass [10, 11],

$$ {}_{\mathrm{dCFL}}(q_0;\mathbf{q}) \overset{M_s \le M_s^c}{=} C_5 \begin{pmatrix} {}_{83}1_3 & & \\ & {}_{82}1_4 & \\ & & \begin{matrix} {}_{81} & \\ & {}_{11} \end{matrix} \end{pmatrix} : \tag{5} $$

In this parameterization, the $SU(3)_{C+V}$ symmetric CFL phase and $SU(2)_C$ $SU(2)_F$ symmetric 2SC phase are expressed only as different limits of the dCFL phase which is invariant under color flavor simultaneous rotation $SU(2)_{C+V}$. We introduce the 5-dimensional vector $\tilde{} = ({}_{83}; {}_{82}; {}_{81}; ; {}_{11})^t$. Using this notation, the model space for the pure CFL state can be expressed by the gap parameter $\tilde{}_{\mathrm{CFL}} = ({}_8; {}_8; {}_8; 0; {}_1)^t$, which spans a 2-parameter section of the full model space. On the other hand, the 2SC phase is characterized by the 1-parameter vector $\tilde{}_{2SC} = ({}_{2SC}; 0; {}_{2SC}=3; \sqrt{2}\,{}_{2SC}=3; 2\,{}_{2SC}=3)^t$.

Propagators. The anomalous propagator is defined by the off-diagonal element of the Nambu-Gor'kov propagator,

$$ \langle T\, q\ (x) q\ (y)\rangle = i \int \frac{d^4q}{(2\ )^4} e^{\ iq(x\ y)} S_{12}\ (q); \tag{6} $$

where S_{12} takes the following form for our ansatz Eq. (5),

$$ S_{12}\ (q) = {}_5 C \begin{pmatrix} R_{83}1_3 & & \\ & R_{82}1_4 & \\ & & \begin{matrix} R_{81} & R \\ R & R_{11} \end{matrix} \end{pmatrix} : \tag{7} $$

Here, $R_{81}({}_{81}; ; {}_{11})$, $R({}_{81}; ; {}_{11})$ and $R_{11}({}_{81}; ; {}_{11})$ are complicated functions of $(\tilde{}; ; M_s)$, some of which we summarize in the appendix.

Gap equations. The gap equation (the Schwinger-Dyson equation) is obtained by using Feynman rule for the self consistency between proposed self-energy and the one-loop self-energy.

$$ i\ \ (p) = \int \frac{d^4q}{(2\ )^4} (\ ig({}^t)\ \ (T^a)^t\ )iS_{12}\ (q)(ig\ \ (T^a)\ \ )iD\ \ (q\ \ p): \tag{8} $$

The bare vertex in the color-flavor mixed base is defined by $(T^a)\ \ = \mathrm{tr}[\ \ {}_a\ ]/4$. $D\ \ (q\ \ p)$ is the gluon propagator. By putting $D\ \ (q\ \ p) \to \ \ g$, we arrive at the gap equation for the NJL model with the vertex for one-gluon exchange $L_{\mathrm{int}} = (1/2)g^2 q\ \ t^a q q\ \ t^a q$,

$$ = i4g^2 \int \frac{d^4q}{(2\ )^4} (T^a)\ \ S_{12}\ (q)(T^a)\ \ : \tag{9} $$

This integral matrix equation contains the following set of five equations.

$$ {}_{83} = g^2 \frac{1}{12}\ \ 5R_{83}\ \ R_{81}\ \ \sqrt{2}\,\sqrt{2}R\ \ \ 2R_{11}\ ; \tag{10} $$

$$ {}_{82} = g^2 \frac{1}{12}\ \ 2R_{82} + 2R_{81} + \sqrt{2}\,\sqrt{2}R\ \ \ 2R_{11}\ ; \tag{11} $$

$$ {}_{81} = g^2 \frac{1}{12}\ \ \ 3R_{83} + 8R_{82}\ \ R_{81} + 2\sqrt{2}\,\sqrt{2}R\ \ \ 2R_{11}\ ; \tag{12} $$

$$ = g^2 \frac{\sqrt{2}}{12}\ \ \ 3R_{83} + 2R_{82} + R_{81}\ \ \sqrt{2}\,\sqrt{2}R\ \ ; \tag{13} $$

$$ {}_{11} = g^2 \frac{1}{6}\ \ \ 3R_{83}\ \ 4R_{82}\ \ R_{81}\ : \tag{14} $$

Here, we have defined $\{R\ \}$ by

$$ R_{\ i}(\tilde{};M_{\ s}) = i \int \frac{d^4q}{(2\ )^4} \frac{1}{4} \mathrm{tr}\left[C\ {}_5 R_{\ i}(q;\tilde{};M_{\ s}) \right] : \tag{15} $$

conversely, the Eqs. (10) (14) can be inverted into the following set of the equations by solving $f R_{83}; R_{82}; R_{81}; R_{11} g$ formally as a function of the gap parameters $\tilde{}$,

$$\frac{3}{8g^2}\left({}_{83} \quad {}_{81} \quad \sqrt{2}\,{}_{11}\right) = R_{83}(\tilde{};M_s); \tag{16}$$

$$\frac{3}{8g^2}\left(2\,{}_{82} + 2\,{}_{81} + \sqrt{2}\,{}_{11}\right) = R_{82}(\tilde{};M_s); \tag{17}$$

$$\frac{3}{8g^2}\left(3\,{}_{83} + 8\,{}_{2} \quad 5\,{}_{81} + 2\sqrt{2}\,{}_{11}\right) = R_{81}(\tilde{};M_s); \tag{18}$$

$$\frac{3\sqrt{2}}{8g^2}\left(3\,{}_{83} \quad 2\,{}_{82} \quad {}_{81} + 3\sqrt{2}\right) = R_{}(\tilde{};M_s); \tag{19}$$

$$\frac{3}{4g^2}\left(3\,{}_{83} + 4\,{}_{82} + 2\,{}_{81} + 2\,{}_{11}\right) = R_{11}(\tilde{};M_s): \tag{20}$$

We should show in the next section that each of these equations is nothing but the derivative of the effective potential in terms of corresponding gap parameter.

B. Effective potential for multi-gap parameters

In this section, we specify our model in detail in order to obtain the expression of the effective potential by applying the Pauli construction. We start from the NJL Hamiltonian density in the color–flavor mixed base:

$$H \quad N = q^{+}\left\{ i\tilde{} \quad r \quad \right) + M \quad {}_0 g q + H_{int:}; \tag{21}$$

with the interaction with one-gluon exchange vertex:

$$H_{int:} \quad \frac{1}{2}g^2 \sum_{a=1}^{8} (q \ (T^a) \quad q \ )(q \ (T^a) \quad q \ ): \tag{22}$$

Here we have defined $\tilde{} \quad {}_0\tilde{}$. The mean field approximation (MFA) can be made by putting the CFL-2SC interpolating ansatz for $hqqi$ correlation,

$$hq_i q_j i = (C \ {}_5)_{ij} \quad ; \quad hq_i q_j i = \quad ({}_5 C)_{ij} \ ^{+} \quad : \tag{23}$$

The Greek character $(i; j; \ )$ should be regarded as spinor indices. We define the quantities having the dimension of energy as

$$= 4g^2 (T^a) \quad (T^a) \quad : \tag{24}$$

$f \ {}_i g$ can be determined uniquely by $f \ {}_i g$. The MFA is made through the procedure:

$$2H_{int:} \ ^{MFA}! \quad (q_i q_k) \quad ({}_5 C)_{ik} + (h:c:) + 4tr_{CF} \ ^{+} \quad : \tag{25}$$

If we assume the CFL-2SC interpolating ansatz for the condensate matrix form of and the gap parameter matrix as

$$= \begin{pmatrix} {}_{83}1_3 & & \\ & {}_{82}1_4 & \\ & & {}_{81} \end{pmatrix}; \quad = \begin{pmatrix} {}_{83}1_3 & & \\ & {}_{82}1_4 & \\ & & {}_{81} \end{pmatrix}: \tag{26}$$

$\tilde{} = (\ {}_{83}; \ {}_{82}; \ {}_{81}; \ ; \ {}_{11})^t$ and $\tilde{} = (\ {}_{83}; \ {}_{82}; \ {}_{81}; \ ; \ {}_{11})^t$ are related by Eq. (24), which leads to

$$\tilde{} = \frac{3}{8g^2}\hat{A}\tilde{}; \tag{27}$$

where the matrix $\hat{A}$ relating the condensates to the gap parameters is defined as

$$\hat{A} = \begin{pmatrix} 0 & 1 & 0 & 1 & \sqrt{2}\sqrt{2} & 2 \\ 1 & 0 & 2 & 2 & \sqrt{2} & 2 \\ \sqrt{3}\sqrt{2} & 2\sqrt{2} & \sqrt{2} & 5 & 2\sqrt{2} & 2 \\ 6 & 8 & 2 & 0 & 6 & 0 \\ 6 & 8 & 2 & 0 & 4 & \end{pmatrix} : \tag{28}$$

Using this matrix $\hat{A}$, the gap equations derived in the previous section can be expressed simply as

$$\tilde{} = \frac{3}{8g^2}\hat{A}\tilde{} \quad \vec{R}[\tilde{};M_s]; \tag{29}$$

with the definition $\vec{R} = (R_{83};R_{82};R_{81};R_{8};R_{11})$, where the kernels $\{R_i\}$ are defined by Eq. (15).

Pauli construction of the effective potential. We use the Pauli trick [2] to derive Effective potential with help of the gap equations.

$$\frac{}{g^2} = \frac{1}{g^2}\langle H_{int}\rangle = \frac{3}{4g^4}(\tilde{};\hat{B}\hat{A}\tilde{}): \tag{30}$$

Here $\hat{B}$ is degeneracy matrix $\hat{B} = \mathrm{diag}:(3;4;1;2;1)$, and $(\ ;\ )$ represents the inner product defined in 5-gap parameter space as $(\vec{A};\vec{B}) \sum_{i=1}^{5} A_iB_i$. Note that $\hat{B}\hat{A}$ is a real-valued symmetric matrix. By integrating over the variable g^2 from 0 to g^2, we obtain the effective potential relative to the naive Fermi gas of 2 massless (u;d) quarks and strange quark with mass M_s, namely $_{e}\ ;\tilde{};M_s$ $\ ;\tilde{};M_s$ $_{0}^{2+1}\ ;M_s$,

$$\begin{aligned} {}_{e}\ ;\tilde{};M_s &= \int_0^{g^2} dg^2\ \frac{3}{4g^4}(\tilde{};\hat{B}\hat{A}\tilde{}) \\ &= \frac{3}{4g^2}(\tilde{};\hat{B}\hat{A}\tilde{}) \int_0^{g^2} dg^2\ \frac{\tilde{}}{g^2};\frac{3}{2g^2}\hat{B}\hat{A}\tilde{} \\ &= \frac{3}{4g^2}(\tilde{};\hat{B}\hat{A}\tilde{}) \quad 4\int_0^{\tilde{}} \tilde{};\hat{B}\vec{R}[\tilde{};M_s] : \end{aligned} \tag{31}$$

Here, we have defined $\tilde{} = (_{83};\ _{82};\ _{81};\ ;\ _{11})^t$. Second line to third line, we have used the gap equation

$$\hat{A}\tilde{} = \frac{8}{3}g^2\vec{R}[\tilde{};M_s]; \tag{32}$$

with the degeneracy matrix $\hat{B} = \mathrm{diag}:(3;4;1;2;1)$. Also the one to one correspondence between g^2 and $\tilde{}$ is assumed. Eq. (31) is a formula of the effective potential, when the kernel of the gap equation is already known. The second term in Eq. (31) represents the condensation energy. We can easily check the fact that the first derivative of the effective potential is equivalent with the gap equation:

$$\hat{B}^{1}\frac{}{\tilde{}} = \frac{3}{2g^2}\hat{A}\tilde{} \quad 4\vec{R}[\tilde{}] = 0: \tag{33}$$

What should be stressed here is that the derivative of the effective potential is not exactly of the same form as the original gap equations set Eqs. (10) (14), but coincides with some linear combinations of those, namely Eqs. (16) (20). This means that we might miss the true effective potential if we construct it from the integral of the original kernel in Eqs. (10) (14). The second term in Eq. (31) corresponding to condensation energy is hard to evaluate the gap-integral except for the iso-triplet and iso-doublet blocks, namely the integral containing R_{83} and R_{82}. Thus we shall try to

---

[2] The author is thankful to T. Kunihiro who suggested me to use this method to construct the effective potential taking care of the multiplicity of the gap parameter.

evaluate these numerically. However, there are two cases in which the effective potential can be written in simple forms, which we summarize in the appendix.

Grand potential. The effective potential Eq. (31) reduces to the following form when is evaluated at the solution $\tilde{}_{sol} = (g; ; M_s)$ of the gap equation Eq. (29)

$$_{cond.}(; M_s) \quad e\,[; \tilde{}_{sol}; M_s] = 2(\tilde{}_{sol}; \hat{BR}[\tilde{}_{sol}; M_s]) \quad 4 \int_0^{\tilde{}_{sol}} \tilde{}\,; \hat{BR}[\tilde{}; M_s] : \tag{34}$$

This is the (thermodynamic) grand potential relative to the naive Fermi gas with (u;d;s). This quantity depends on (;T;M_s), and its derivative in terms of (;T) is nothing but ($_{rel}$;S_{rel}), namely the quark density and the entropy relative to the simple Fermi gas. This formula Eq. (34) is useful because the coupling g^2 does not enters this formula explicitly, but does implicitly through the gap $\tilde{}_{sol}$.

III. NUMERICAL RESULTS

Here, we present our numerical results. The cutoff parameter is set to = 800MeV, and the coupling parameter g^2 is tuned to reproduce 400MeV for the constituent mass of quark at zero chemical potential [11]. We have checked all of the main results here are robust against the variation of the cutoff parameter.

A. Solution of gap equation

We here discuss the solution of the coupled gap equation Eqs. (16) (20) as a function of strange quark mass M_s. In FIG. 1(a), we show the eigenvalues of the original gap matrix Eq. (5) as functions of M_s. ($_{83}$; $_{82}$) are the gaps for iso-triplet and doublet fermionic excitations. ($_1$; $_2$) are the eigenvalues of the iso-singlet mixed sector, $_{1(2)} = \frac{1}{2}\,(\,_{81} + \,_{11}) \mp \sqrt{(\,_{81} - \,_{11})^2 + 4\,^2}$. In the pure CFL state, ($_1$; $_2$) = (j $_1$j;j $_8$j), and in the 2SC state, ($_1$; $_2$) = (j $_{2SC}$j;0). However, we note that in the distorted CFL state for moderate M_s, the true gaps for the fermionic excitation is defined by more complicated functions of (;M_s; $_{81}$; ; $_{11}$;M_s), which are the minimums of two dispersion $z_{1;2}$(p; ; $_{81}$; ; $_{11}$;M_s), namely the solutions of the quartic algebraic equation which we give explicitly in Eq. (A4). According to the values of these parameters, the states are distinguished by

Gap parameters	Global Symmetry	States
$_{83} = \,_{82} = \,_2$; $_1 \neq 0$	$SU(3)_V$	CFL for $M_s = 0$
$_{83} = \,_1$; $_{82} = \,_2 = 0$	$SU(2)_L \quad SU(2)_k$	2SC for $M_s > M_s^c$
otherwise	$SU(2)_V$	distorted CFL (dCFL)

It is surprising that the system stays in the distorted CFL (dCFL) phase even for $M_s \gg = 400$ MeV. This should be contrasted with the $M_s^c \quad 240$ MeV and $M_s^c \quad \sqrt{\,_8(M_s = 0)} = 180$ MeV from a kinematical criterion for unlocking [11]. In FIG. 1(b), we display the gaps ($_{83}$; $_{82}$; $_1$; $_2$) for $M_s = 250$ MeV as functions of temperature. We see that as the temperature is raised, the dCFL phase encounters the continuous transition to the 2SC state at T = 35MeV, and eventually the system undergoes 2nd order phase transition to the normal fermi-liquid at T = 60MeV.

In order to see aspects of the phase transition to the 2SC state with increasing M_s or T in more detail, we study the bulk quantities as well as the gaps. In FIG. 1(c), we show the grand potential relative to the non-interacting gas with two massless (u;d) quarks and s quark with mass M_s, namely $_{cond.}(; M_s) = P(; M_s) \quad P_0^{2+1}(; M_s)$ (see Eq. (34)) in the unit of the pressure of the massless 3 flavor normal Fermi gas $P_0^{3f}( ) = 3\,^4/4\,^2$. In the chiral limit, the system is the pure CFL state. As one increases the strange quark mass M_s, the grand potential gradually decreased, and saturates to the value for the 2SC state. The condensation energy for the pure CFL state is almost 1.9 times as large as that for the 2SC state, which is consistent with the weak coupling analysis [18] and also with Schwinger-Dyson approach [19]. From this figure, it is still not clear whether the unlocking transition at T = 0 is of continuous 2nd order or higher order, or even the smooth crossover (The CFL never unlocks into the 2SC). In any case, our results contradict those obtained in previous work [10, 11]. In FIG. 1(d), $_{cond.}(; T; M_s)/P_0^{3f}( )$ is plotted as a function of T, for strange quark masses M_s = 0 (pure CFL);200;250;300;1 (2SC). The critical temperatures of the transition to normal fermi gas are all the same (T_c = 60 MeV) for all values of the strange quark mass [19]. The grand potential for all values of M_s approaches the 2SC curve towards some temperature $T_c^{unlock}(M_s) < T_c$, at which the continuous unlocking transition occurs. This unlocking critical temperature $T_c^{unlock}(M_s)$ is the decreasing function of M_s. This

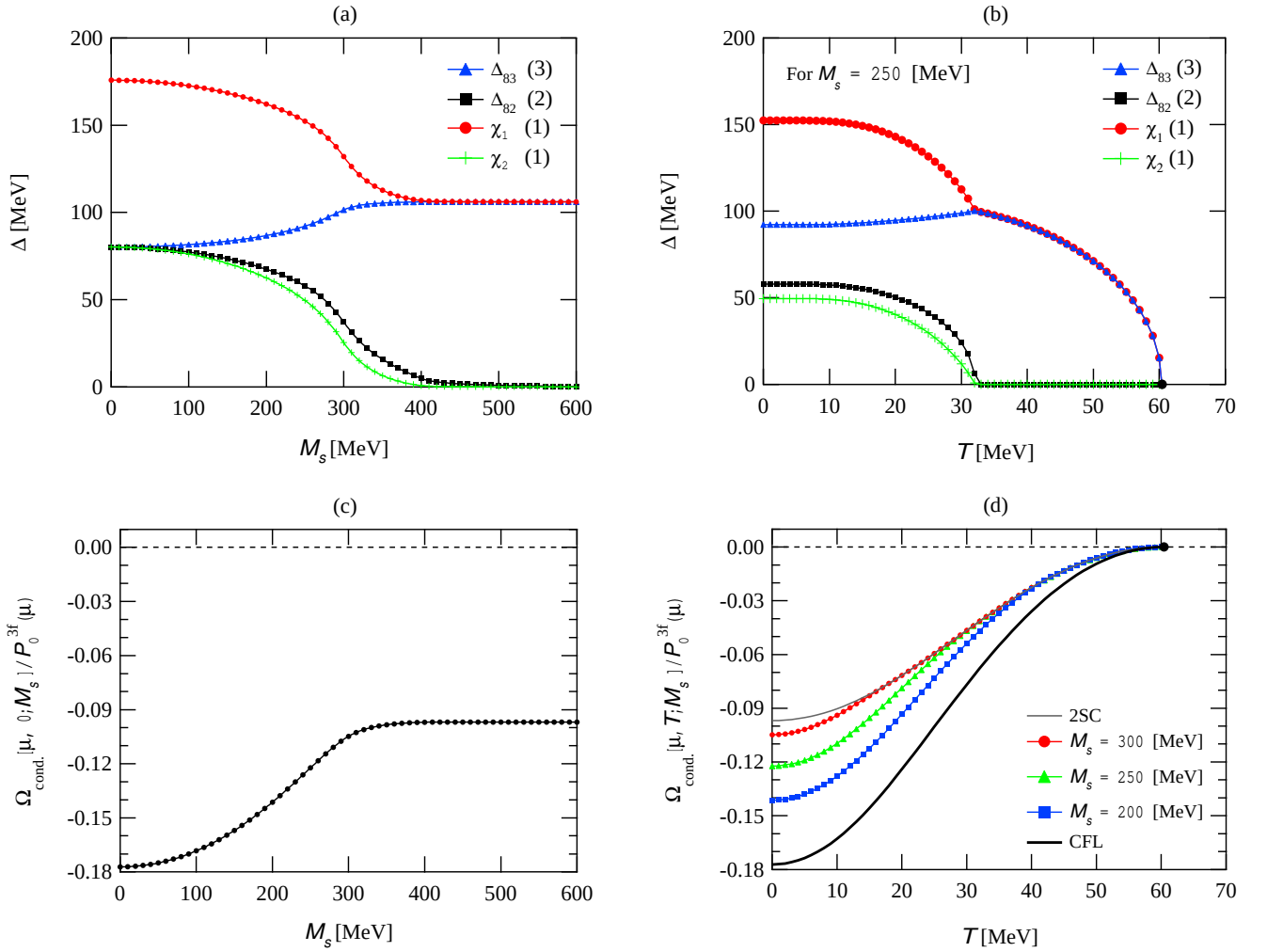

FIG. 1: (a) Gaps are plotted as functions of M_s. (b) The temperature dependence of the gaps for $M_s = 250$ MeV. (c) The grand potential of the pairing state relative to the non-interacting Fermi gas with (u;d;s) quarks is plotted as a function of M_s. (d) The grand potential as a function of T for $M_s = 0$ (the CFL state), $M_s = 200;250;300$ MeV and for M_s (the 2SC state).

is because the energy gain of the CFL state relative to the 2SC state gets smaller with increasing M_s, as is clear from FIG. 1(c). We discuss the $(M_s; T_c^{unlock})$ relation in more detail later.

Continuous 2nd order unlocking or absence of unlocking? We found that the unlocking for nite temperature is of 2nd order, but this becomes rather ambiguous at zero temperature. In FIG. 2, we display the $_{82}$ gaps, the order parameter for the unlocking transition, as a function of M_s for various temperatures. Here again we con rm that the unlocking for nite temperature is of continuous 2nd order. The strength of 2nd order transition seems to get weaker as one decreases temperature. However, we cannot determine the order of unlocking transition for $T = 0$ due to possible numerical errors for M_s = 800 MeV. There arise two likely possibilities: (1) the asymptotic smooth unlocking and (2) the continuous second order phase transition. (1) means that the CFL never gets unlocked into the 2SC as long as the value of the strange quark mass stays nite, and (2) corresponds to the case that the CFL state gets unlocked into the 2SC with weak 2nd order transition at some nite critical value of M_s. Only a solid fact is that the CFL pairs become more and more sti against increase of M_s with decreasing T.

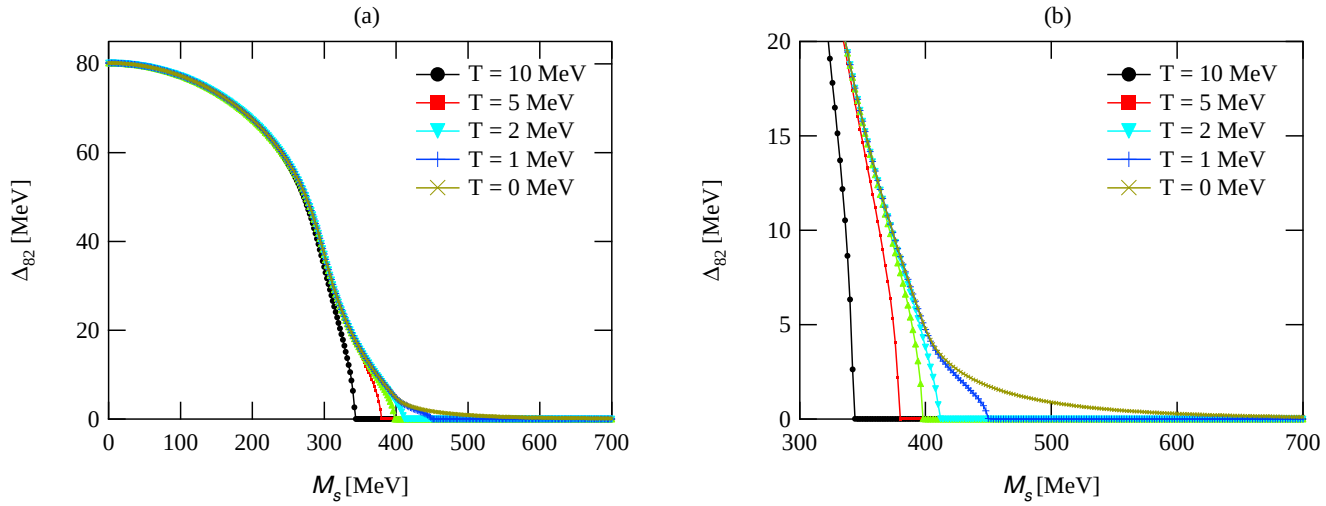

FIG. 2: (a) The gaps are plotted as a function of strange quark mass for various values of temperature. (b) Just an enlargement of (a) near the critical masses for unlocking.

B. Effective potential for multi-gap parameter space

In the previous section, we saw that the CFL state is always stable relative to the 2SC state for M_s. by analyzing the grand potential. Now, by computing the effective potential with help of the formula Eq. (31), we study how these states are realized in the multi-gap parameter space, and want to discuss the unlocking at zero temperature in more detail. In FIG. 3, we display the effective potential $_e$ [~;M_s] in the section spanned by the 2SC gap ~$_{2SC}$ = (106;0; 35; 50; 70) MeV and the CFL gap ~$_{CFL}$ = (80;80;80;80; 175) MeV. By introducing the vector ~(i;j) = $\frac{(i\ 10)\tilde{}_{CFL} + (j\ 10)\tilde{}_{2SC}}{50}$; we define 2-dimensional planer section in the 5-dimensional gap parameter space, which includes the simple Fermi gas (10;10) with ~ = 0, the CFL (60;10) and the 2SC (10;60). In FIG. 3, the values of the effective potential $_e$ [~(i;j)] are contoured as a function of (i;j) for M_s = 0 MeV (a), 200 MeV (b), 300 MeV (c) and 400 MeV (d). We can see that the CFL state (60;10) looks the global minimum in this 2-parameter space (i;j) for M_s = 0 MeV. On the other hand, the 2SC state (10;60) is realized as a saddle point which is stable in the direction of the simple Fermi gas (10;10), but is unstable in the direction towards the CFL state (60;10). As the strange quark mass is increased to 200 MeV, the CFL minimum moves towards the 2SC point, and its condensation energy gets reduced, while the position and the energy of the 2SC state is unaffected by M_s. This minimum point (55;20) corresponds to the distorted CFL state [3]. The dCFL state gets distorted significantly towards the 2SC state at M_s = 300 MeV (FIG. 3(c)), and seems absorbed into the 2SC as the strange quark mass approaches the order of the chemical potential of the system. We can see that the unlocking at T = 0 is likely of 2nd order, but still cannot exclude a possibility of the absence of the unlocking itself.

2SC as a solution of gap equation. What should be stressed here is that the 2SC stays at least a saddle point in the full model space irrespective of the value of M_s. This means that the 2SC is always a solution of the gap equation, and if we had missed in obtaining the correct effective potential, then we misunderstood it as the true ground state instead of the dCFL state for intermediate strange quark mass M_s.

Unstable CFL vacuum. In FIG. 4(a), we plot the section of the effective potential surface FIG. 3(a) on the line linking the 2SC (10;60) ~$_{t=0}$ = ~$_{2SC}$ and the CFL (60;10) ~$_{t=1}$ = ~$_{CFL}$. Both states are determined by solving the gap equation in 5-gap parameter space for M_s = 0 MeV. Now we address the question whether the CFL state is true global minimum even in the full model space or not. FIG. 4(b) shows us the answer for this question. Five potential

[3] Strictly speaking, it is not necessary that this point does exactly coincide with the true dCFL point, because we restrict ourselves to drawing the effective potential even in the 2-dimensional planer in the 5-parameter space. But it is sufficient here to mention that the dCFL state other than the 2SC state exists near the point (55;20) in full model space, and indeed, it has a larger condensation energy than the 2SC state.

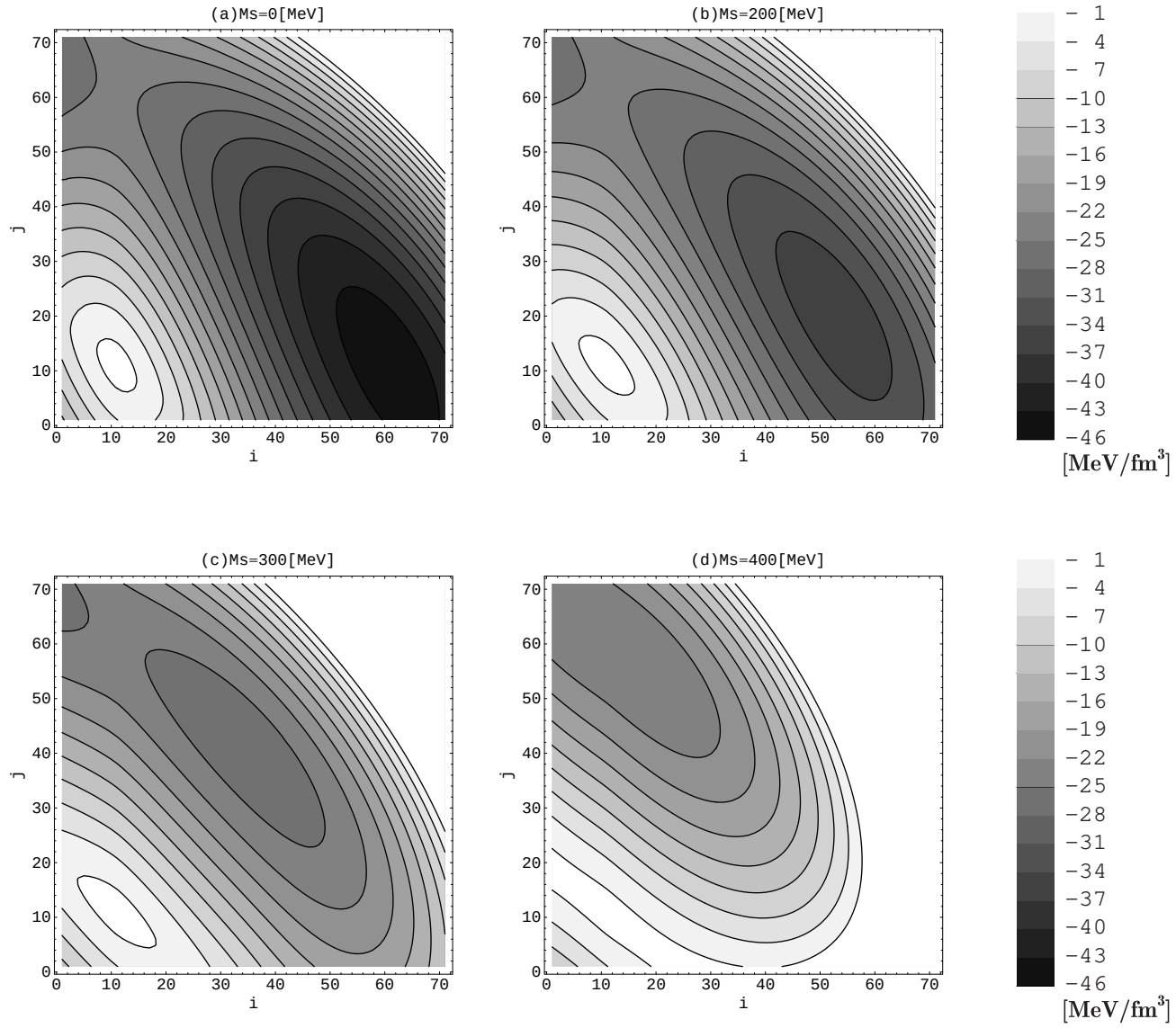

FIG. 3: Contour plot of the effective potential for $(T;\mu) = (0;400)$ MeV in the 2-dimensional sector spaned by the CFL gap vector $\tilde{\Delta}_{CFL} = (80;80;80;80;\ 175)$ MeV and the 2SC gap vector $\tilde{\Delta}_{2SC} = (106;0;\ 35;\ 50;\ 70)$ MeV. Effective potential surface for $M_s = 0$ MeV (a), $M_s = 200$ MeV (b), $M_s = 300$ MeV (c), and for $M_s = 400$ MeV (d). In figure, the point $(i;j) = (10;10)$ corresponds to the normal fermi gas with 2 massless flavor and 1 massive strange quark. The points (60;10) and (10;60) corresponds to the pure CFL state and the 2SC state, respectively.

curves are shown near the pure CFL for $M_s = 0$, each of which represents the potential curve in the direction of an eigenvector belonging to the corresponding eigenvalue of the Hessian curvature matrix at the CFL point:

$$\frac{\partial^2}{\partial\ \tilde{\Delta}_i \partial\ \tilde{\Delta}_j}\Bigg|_{\tilde{\Delta}=\tilde{\Delta}_{CFL}} = \left[\frac{3}{2g^2}(\hat{B}\hat{A})_{ji} - 4\hat{B}_{jl}\frac{\partial R_l[\tilde{\Delta}]}{\partial\ \tilde{\Delta}_i}\right]_{\tilde{\Delta}=\tilde{\Delta}_{CFL}} : \tag{35}$$

What is surprising is that the CFL state is not the global minimum in the full model space, and seems unstable in three out of five directions. These three directions correspond to the color-flavor sextet channels in which the interaction acts repulsive, as we show explicitly this fact in the appendix. FIG. 5 shows the effective potential on the line which connects $\tilde{\Delta} = (80;80;80;80;175)$ [MeV] and $\tilde{\Delta}_A = (84;84;84;84;168)$ [MeV]. $\tilde{\Delta}$ is the CFL solution in the full (5-dimensional) model space, while the $\tilde{\Delta}_A$ is a solution of the gap equation in 2-dimensinal plane specified by

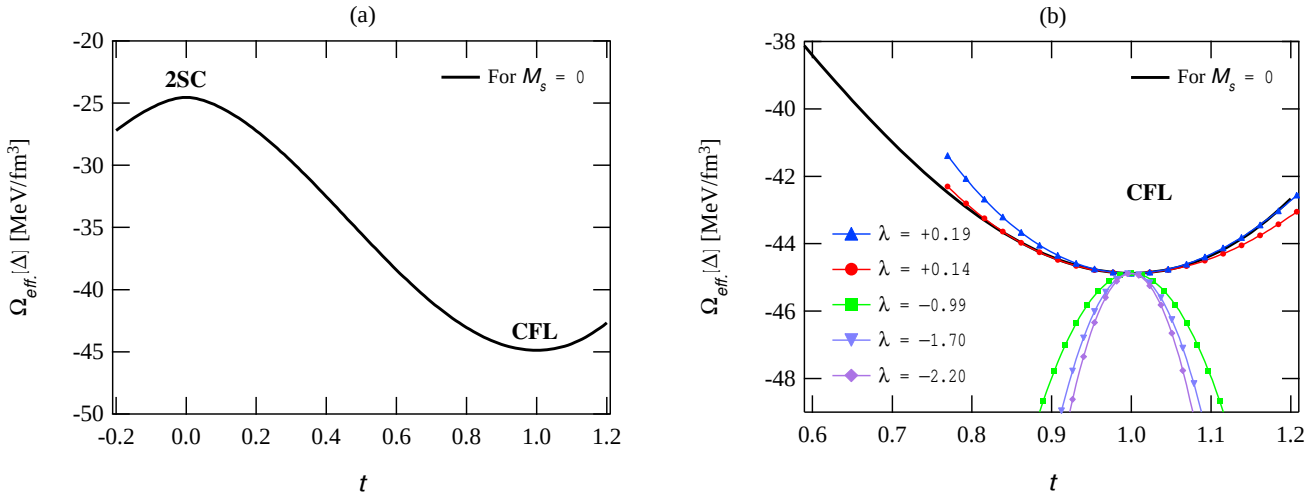

FIG. 4: (a) The values of the effective potential on the 1-dimensional line connecting from the 2SC state $t = 0$ to the CFL state $t = 1$. (b) The bold line is just an enlargement of the potential curve for $M_s = 0$ in (a), and five sets of the points (triangles, bold dots, squares, reflected triangles, lozenges) represent the potential curves in the directions of the eigenvectors belonging to the five eigenvalues $= (0.19; 0.14; 0.99; 1.70; 2.20)^2$ of the Hessian curvature matrix at the CFL.

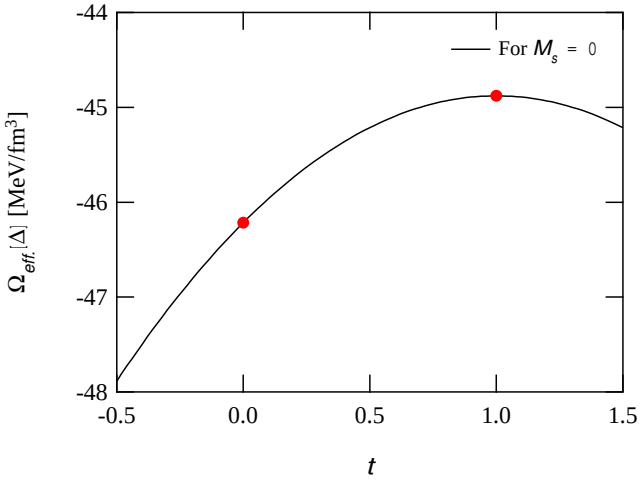

FIG. 5: The effective potential $_e$ $[(1 \quad t)\tilde{}_A + t\tilde{}]$ is plotted as a function of t. $t = 0$ (1) corresponds to the solution in the 2-dimensional plane for anti-triplet gap (in the full model space).

Eq. B 9, the 3-constraints which guarantee the vanishment of color symmetric gaps. The gap equation in restricted anti-symmetric space is given by

$$\frac{@}{@ \ _{83}} ; \frac{@}{@ \ _{82}} \quad _e [\ _{83}t + \ _{82}s] = (0; 0);$$

with the definition $t = (1; 0; \ 1=3; \ \overline{2=3}\,\overline{\ }\,)$ and $s = (0; 1; 4=3; \ \overline{2=3}\,\overline{\ }\,)$, two bases for anti-symmetric gap parameter space. We can see three facts: (1) including symmetric components into gap equation yields only small difference of order 5 10 MeV, (2) the energy for the solution restricted in the 2 parameter space actually has a smaller energy than that in full model space, and (3) the solution in 2 parameter space is not a saddle point in the full space with finite slopes in the color sextet directions. (1) is consistent with results obtained in old work, while (2) and (3) have not been noticed yet. It is often said that sextet gaps are induced non-perturbatively by the condensation in anti-triplet channels. However, the facts (2) and (3) show that this statement is misleading because the effective potential has a uphill slope at $\tilde{}_A$ in the direction of the full solution with sextet condensations.

Anyway, because of the existence of repulsive force in the sextet channels, the corresponding ladder (RPA) modes

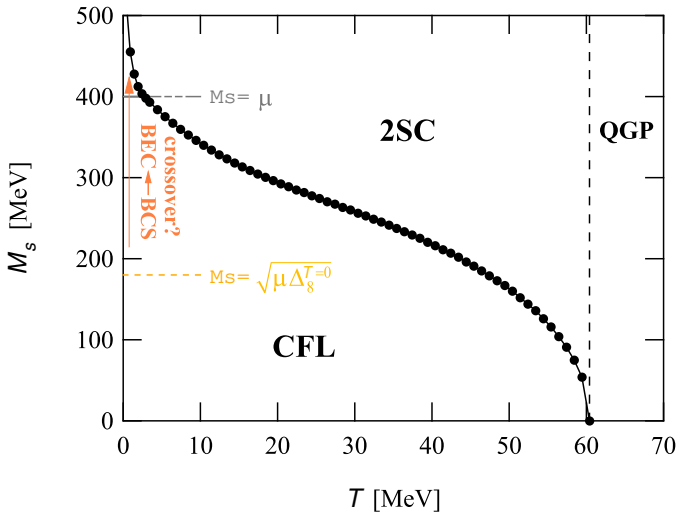

FIG. 6: Phase diagram in $(T; M_s)$ plane for $= 400$ MeV. Bold dots represent the color-flavor unlocking line separating the superconducting area into the dCFL and 2SC phases, while the dashed line $T \quad 60$ MeV is a phase boundary between the 2SC phase and the normal Fermi gas.

are actually heavy (not tachyonic), it makes no physical sense to include symmetric mean fields contribution [4, 20, 21] in the ansatz for the gap matrix from the beginning[4].

C. Phase diagrams

We here show two phase diagrams determined by constructing the effective potential for multi-gap parameters. In FIG. 6, we show the phase diagram in $(T; M_s)$ plane. At $M_s = 0$, we have the CFL phase for $T < T_c$, and the normal fermi gas phase for $T > T_c$. Both phases are divided by 2nd order phase transition. As the strange quark mass is increased, we have three phases according to the region of temperature, the dCFL phase for low temperature $T < T_c^{unlock}$, the 2SC phase for $T_c^{unlock} < T < T_c$, and the normal Fermi gas of quarks for $T > T_c$. These three phases are divided by 2nd order phase transition. T_c^{unlock} is the deacreasing function as increasing strange quark mass, while T_c is unaffected by the increase of M_s. The former results from the smaller condensation energy for dCFL state as increasing M_s, and the latter is attributed to the fact that the the parameter M_s is completely decoupled from the 2SC gap equation. $T_c^{unlock} = 35$ MeV at $M_s = 250$ MeV, which we saw exactly in FIG. 1(b). As we have discussed in the previous section, the dCFL phase exists for $M_s >$. This situation is similar to the crossover from the BCS to the Bose-Einsteint condensation (BEC) in the non-relativistic fermion systems [22, 23, 24], where the condensed phase with phase coherence continues from the weak coupling (dense) BCS state to the strong coupling (dilute) BEC state with negative value of the chemical potential. The BCS-BEC crossover from relativistic weak coupling CFL state to the strong coupling CFL BEC state might be realized in our case. The crossover phenomena in the relativistic systems are also widely studied in relation to the chiral phase transition [25], in the 2-flavor color superconductor [26] and in the 2-color QCD [27]. If this BCS-BEC crossover is acually the case, we would have the pair dissociation line above the unlocking line for the region of large strange quark mass, and which may also provide another description of so-called "pseudo gap" phase [28, 29]. We will examine the possibility of the BCS-BEC crossover scenario in more detail elsewhere.

Finally, we show the phase diagrams in the entire $(; T)$ plane in FIG. 7. FIG. 7(a) shows the phase diagram for $M_s = 400$ MeV. The squares represent the color-flavor unlocking line on which the CFL (2SC) state turns into the 2SC (CFL) phase. We can see clearly that our CFL phase is much more robust than that obtained through the kinematical criterion which says, if the strange quark mass is increased so that the mismatch of Fermi momenta of two species exceed the value: $\sqrt{\quad^2 \quad M_s^2} = \frac{M_s^2}{2} \& 2j_{\ 8}(T)j_{M_s=0}$, then the CFL gets unlocked to the 2SC phase

[4] It might also be worth mentioning that the color-flavor sextet gap parameters do not break any symmetry, thus are not order parameters for the unlocking as is anticipated in their critical behaviour $(1 \quad T=T_c)^{3=2}$ near critical temperature T_c in the chiral limit [19].

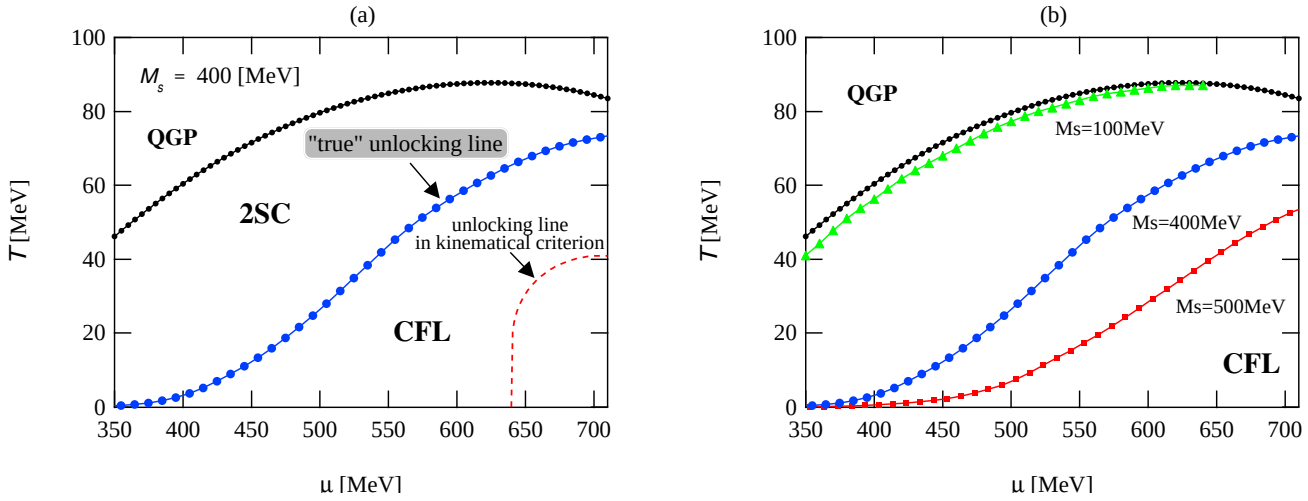

FIG. 7: (a) Phase diagram in (;T) plane for $M_s = 400$ MeV. The bold dots represent the phase boundary between the 2SC and QGP phases. This is characterized by 2nd order phase transition. The squares are the color- avor unlocking line for $M_s = 400$ MeV. This divides the superconducting region into the upper 2SC phase and the lower CFL phase by 2nd order phase transition. The dashed line shows a unlocking line evaluated with a simple kinematical criterion. (b) The color avor unlocking lines for $M_s = 100$ MeV (triangles), 400 MeV (bold dots), and 500 MeV (squares).

by 1st order phase transition. The order of the phase transition is 2nd order as we discussed, which also contradicts the simple kinematical picture for the unlocking. The region . $M_s = 400$ MeV, we still have a slight region for dCFL phase at $T < T_c^{unlock}(M_s = 400;)$ T_c. In this region, we expect the BEC like state with tightly bound CFL diquarks, and above which we might have a possible pseudogap phase of thermal Bose gas.

In FIG. 7(b), we show the unlocking line and its dependence upon the strange quark mass. Though we have not included the usual vacuum e ect of chiral symmetry breaking due to non vanishing hqqi, but once it is included, we might have one line in (;T) plane, on which the qq condensates show singular behaviours [30, 31]. However, this e ect enters the superconducting gap equation only through shifts of the quark masses. If the usual chiral restoration occurs at = 450 MeV, we still might have the CFL phase above this point for signi cantly larger value of in-medium strange quark mass: M_s . 500 MeV, as is easily guessed from the squares in FIG. 7(b). If this case, the chiral symmetry is always broken at $T = 0$ regardless of the value of the chemical potential [32]. Buballa and Oertel had shown that the 2SC/CFL transition gets triggered by the sudden jump in the strange quark mass at $_c^{II}$ located much above usual chiral restoration ($SU(2)_V$! $SU(2)_R$ $SU(2)_L$) point $_c^{I}$ ($_c^{I} < _c^{II}$) [33, 34]. However, this 1st order like discontinuity in the strange quark mass at $_c^{II}$ is rather related to the only approximate $U_s(1)$ "chiral" symmetry in strange quark sector. This symmetry is violated signi cantly by bare strange quark mass m_s, and there is theoretically a very large possibility of 1st order transition (strong coupling, small bare strange quark mass) and smooth crossover (weak coupling, large bare strange quark mass), and a ultimately small (point-like) possibility of 2nd order transition, even though they obtained 1st order transition for a set of model parameters. In addition, the transition point they obtained is located very close to the cuto parameter. In these reasons, the 1st order phase transition might be an artifact of NJL-type cuto model. If this transition is of smooth crossover in real world, which means, in-medium strange quark mass is a smooth function of , then the results obtained here have a great impact. Flavor mixing due to instanton might bring a discontinuity in the in-medium strange quark mass at $_c^{I}$ corresponding to usual chiral restoration for light avor sector [34, 35], this e ect is expected to be small for nite density, and we can still expect the wide region for color- avor locking phase and no region for restoring the chiral symmetry for $T = 0$.

IV. SUMMARY

In this paper, we have applied the NJL model to study the phases of quark matter under high chemical potential. We have constructed the correct e ective potential for multi-gap parameters including color- avor sextet channels to determine the phase diagram, and which has not yet been taken care in other references. In particular, we have revisited the unlocking phase transition from the CFL to the 2SC. We list main results below.

1. Continuous unlocking or the smooth cross over. The unlocking transition is of continuous weak 2nd order for nite

temperature. Even though it is hard to conclude whether the unlocking is of 2nd order or even it does not take place in spacial case for $T = 0$, the 1st order unlocking never appears. This contradicts the simple kinematical picture for the color-flavor unlocking transition.

2. Toughness of the CFL state. The CFL state at $T = 0$ is much more robust against the increase of M_s than is predicted from the kinematical criterion, and the 2SC state is continuously connected from the dCFL state at the strange quark mass $M_s^c \& (2\sqrt{\Delta_8(\mu; M_s = 0)})$.

3. The 2SC as a saddle point. 2SC state is always a saddle point, a solution of the gap equation, of the effective potential for any value of M_s, which is unstable in the direction towards the dCFL state, as well as three color-flavor sextet directions. The dCFL state, a solution of the gap equation with a larger condensation energy than the 2SC state approaches the 2SC saddle point as M_s approaches M_s^c.

4. Role of the sextet gap parameters. The dCFL state is also unstable in the directions for three color-flavor symmetric channels. This is attributed to the fact that the interaction is repulsive in these channels. We have no reason to include the symmetric components of the gap parameter into our ansatz from the beginning, because no Cooper instability due to tachyonic RPA mode is present in these repulsive channels. However, the effects of the sextet gaps on the anti-triplet sector are very small even if they are included.

In addition to these solid conclusions, we conjecture that the BCS-BEC crossover well-known in the non-relativistic systems might actually take place in the relativistic CFL pairing phase. If the scenario of the crossover is exactly the case, the incoherent Bose gas of pairs might exist above the critical temperature for the unlocking $T_c^{\text{unlock}} < T < T_c$, and which may provide another description of so-called "pseudogap" phase. In order to confirm this picture, we have to study q-q bound state for finite temperature and density. The Bethe-Salpeter equation would be a good starting point to investigate this crossover phenomenon.

In this paper, we completely neglected the electric charge neutrality and also the color neutrality [36, 37]. It would be interesting to study these effect on the gap equation, and to confirm whether our BEC state is robust or fragile to be withdrawn by the neutrality condition. Also, we have ignored the usual chiral condensates in the vacuum. However, we have to include this effect to discuss the phase transitions in the lower chemical potential region. Studying phase transitions in this regime by improving our model along this line is also an interesting subject to be done in the future.

Acknowledgments

I am grateful to T. Kunihiro for critical advices, stimulating discussions and continuous encouragements. I would also like to express my sincere thanks to T.T. Takahashi, M. Kitazawa, H. Matsufuru, N. Ikezi and S. Nakamura for helpful conversations and warm encouragements, and to K. Iida, M. Tachibana, K. Rajagopal, T. Schafer and M.F.M. Lutz for their valuable comments and interests in this work.

APPENDIX A: GAP EQUATIONS

We summarize here some quantities, in particular, the quark propagators and the resulting dispersion relations of the quasi-quarks, both of which are relevant to the calculation of the gap equation and the effective potential.

Propagators. Iso-triplet and iso-doublet sector of the propagator matrix (Eq. (7)) are

$$R_{83}(p; \Delta_{83}) = {}_5C\frac{1}{2}\left[\frac{\Delta_{83}}{p_0^2 - (p - \mu)^2 - \Delta_{83}^2} + (\mu \to -\mu)\right],$$

$$R_{82}(p; \Delta_{82}) = {}_5C\frac{1}{4}\left[\frac{\Delta_{82}}{p_0^2 - (p - \mu)^2 - \Delta_{82}^2} + \frac{\Delta_{82}}{p_0^2 - (\sqrt{p^2 + M_s^2} - \mu)^2 - \Delta_{82}^2} + (\mu \to -\mu)\right].$$

The component of iso-singlet mixing sector, namely $R_{81}(\Delta_{81}; \Delta_{11}), R(\Delta_{81}; \Delta_{11})$ and $R_{11}(\Delta_{81}; \Delta_{11})$ takes very complicated form. For example, $R_{81}(\Delta_{81}; \Delta_{11})$ turns out

$$R_{81}(p; \tilde{}) = {}_5C\frac{\Delta_{81}p_0^6 - A_3(p; M_s; \tilde{})p_0^4 - A_5(p; M_s; \tilde{})p_0^2 - A_7(p; M_s; \tilde{})}{p_0^8 + B_2(p; M_s; \tilde{})p_0^6 + B_4(p; M_s; \tilde{})p_0^4 + B_6(p; M_s; \tilde{})p_0^2 + B_8(p; M_s; \tilde{})};$$

with

$$A_3(p;M_s;\tilde{\ };\ ) = 3\ _{81}(p^2+\ ^2)+\ ^3_{81}\ \ ^2\ _{11}+2\ _{81}(\ ^2+\ ^2_{11})$$
$$+\frac{2}{9}M_s^2\Big\{5\ _{81}+\frac{p}{2}+\ _{11}\Big\};$$

$$A_5(p;M_s;\tilde{\ };\ ) = 3p^4\ _{81}\ \ 2p^2\ ^3_{81}\ \ ^2\ _{11}+\ _{81}2\ ^2+\ ^2_{11}+\ ^2$$
$$+3\ ^2_{81}\ ^2\ _{11}\ \ 2\ ^3_{81}\ \ ^2_{11}+\ ^2+\ ^2\ _{11}2\ ^2+\ ^2_{11}+2\ ^2$$
$$_{81}\ ^2+\ ^2_{11}+\ ^2\ \ ^2+\ ^2_{11}+3\ ^2$$
$$+\frac{M_s^2}{9}\ \ 4p^2\ 5\ _{81}+\frac{p}{2}+\ _{11}\ \ 6\ ^2_{81}\frac{p}{2}+\ _{11}$$
$$+\ _{11}5\ ^2\ \ 2\ ^2_{11}\ \ 4\ ^2\ \ 2\frac{p}{2}\ \ 2\ ^2+\ ^2_{11}\ \ 4\ ^2$$
$$2\ ^3_{81}\ \ 2\ _{81}5\ ^2+4\frac{p}{2}\ _{11}+7\ ^2_{11}+4\ ^2$$
$$+\frac{M_s^4}{9}\Big\{\ _{81}\ \ 2\frac{p}{2}+\ _{11}\Big\};$$

$$A_7(p;M_s;\tilde{\ };\ ) = (\text{complicated terms of energy}^{\ 7});$$

$$B_2(p;M_s;\tilde{\ };\ ) = 2\ 2(p^2+\ ^2)\ ^2_{81}+2\ ^2+\ ^2_{11}\ \ 2M_s^2;$$

$$B_4(p;M_s;\tilde{\ };\ ) = 6p^4+2p^2\ 6\ ^2+3\ ^2_{11}+\ ^2_{81}+2\ ^2+6\ ^4+6\ ^2_{11}+\ ^2_{81}\ ^2$$
$$+6\ ^4+\ ^4_{11}+4\ ^2_{11}\ ^2_{81}+\ ^4_{81}+4\ ^2\ ^2_{11}\ \ _{11}\ _{81}+\ ^2_{81}+3\ ^2$$
$$+\frac{2}{9}M_s^2\Big\{27p^2+9\ ^2+26\ ^2+13\ ^2_{11}+4\ _{11}\ _{81}+10\ ^2_{81}$$
$$+4\frac{p}{2}\ (2\ _{11}+\ _{81})\Big\}+M_s^4;$$

$$B_6(p;M_s;\tilde{\ };\ ) = (\text{complicated terms of energy}^{\ 6});$$

$$B_8(p;M_s;\tilde{\ };\ ) = (\text{complicated terms of energy}^{\ 8}):$$

These propagators reduce to considerably simple forms in the case of the 2SC state and the pure CFL state. For the 2SC state with $_{2SC} = \ 3\ _{81} = \ 3=\frac{p}{2} = \ 3\ _{11}=2$, we have

$$R_{81}(p;\ _{2SC}) = \ _5C\frac{1}{6}\ \frac{^{2SC}}{p_0^2\ \ (p\ \ ^3)\ \ ^2_{2SC}}+\frac{^{2SC}}{p_0^2\ \ (p+\ ^8)\ \ ^2_{2SC}}\ ;$$

and $R(p;\ _{2SC}) = \frac{p}{2}R_{81}(p;\ _{2SC});\ \ R_{11}(p;\ _{2SC}) = 2R_{81}(p;\ _{2SC})$. These do not depend on the value of M_s. As for the pure CFL state with $M_s = 0;\ _{83} = \ _{82} = \ _{81}\ \ _8;\ = 0;\ _{11} = \ _1$, we obtain $R(p;CFL) = 0$, and

$$R_{81}(p;CFL) = \ _5C\frac{1}{2}\ \frac{^8}{p_0^2\ \ (p\ \ ^3)\ \ ^2_8}+\frac{^8}{p_0^2\ \ (p+\ ^8)\ \ ^2_8}\ ;$$
$$R_{11}(p;CFL) = \ _5C\frac{1}{2}\ \frac{^1}{p_0^2\ \ (p\ \ ^3)\ \ ^2_1}+\frac{^1}{p_0^2\ \ (p+\ ^8)\ \ ^2_1}\ :$$

Fermionic dispersion. Fermionic excitation dispersions can be determined by the poles of the quark propagator. We can easily extract the seven low energy dispersions out of nine as

$$d=3\ :\ E_{83} = \sqrt{(p\ \ ^8)^2+\ ^2_{83}};\tag{A1}$$
$$d=2\ :\ E^0_{82} = \sqrt{(p\ \ ^8)^2+\ ^2_{82}};\tag{A2}$$
$$d=2\ :\ E_{82} = \sqrt{\ \sqrt{p^2+M_s^2}\ \ ^2+\ ^2_{82}}:\tag{A3}$$

$E_{83};E^0_{82}$ and E_{82} are the dispersion relation for the iso-triplet, iso-doublet, and iso-doublet excitations, respectively, and d represents the degeneracy of each excitation. Other two dispersions cannot be written in such simple forms. However, in principle, they can be obtained by solving

$$z^4+B_2(p;M_s;\tilde{\ };\ )z^3+B_4(p;M_s;\tilde{\ };\ )z^2+B_6(p;M_s;\tilde{\ };\ )z+B_8(p;M_s;\tilde{\ };\ ) = 0\tag{A4}$$

in variable z from the smallest solution up to two, and putting $E(p) = \sqrt{z}$. There are four solutions in the quadratic equation in general, but other two solutions can be obtained through the procedure $\to$ in the two smaller solution, and which are higher blanches of the dispersions, indeed for the excitation which consist mostly of anti-quarks component.

APPENDIX B: EFFECTIVE POTENTIAL

Here, we explicitly calculate some blocks of the effective potential via the Pauli trick.

Condensation energy. The condensation energy term, the second term of Eq. (31), is hard to calculate the frequency integral except for some blocks. For example, iso-triplet sector, we can calculate as

$$\begin{aligned} 12\int_0^\infty dt\ \Delta_{83} R_{83}[\Delta_{83} t] &= 3\int \frac{dq}{(2\pi)^3}\int_0^\infty dt\left[\sqrt{(q^2+t^2)^2+\Delta_{83}^2}-(q^2+t^2)+\Delta_{83}^2\right] + (\$) \\ &= 3\int \frac{dq}{(2\pi)^3}\left[\sqrt{E_0^2+\Delta_{83}^2}-|E_0|\right] + (\$). \end{aligned}$$

Here, we have defined the bare quark dispersion $E_M = \sqrt{q^2+M^2}$. In the same manner, iso-doublet sector, we obtain

$$\begin{aligned} 16\int_0^\infty dt\ \Delta_{82} R_{82}[\Delta_{82} t] &= 2\int \frac{dq}{(2\pi)^3}\left[\sqrt{E_0^2+\Delta_{82}^2}-|E_0|\right] + (\$) \\ &= 2\int \frac{dq}{(2\pi)^3}\left[\sqrt{E_{M_s}^2+\Delta_{82}^2}-|E_{M_s}|\right] + (\$). \end{aligned}$$

However, it cannot evaluate integral of the singlet mixing sector $R_{81}, R_{\Delta}, R_{11}$ analytically, thus we calculated these numerically.

Mean field potential. The pure CFL state in Eq. (3) can be written in terms of color-flavor anti-symmetric and symmetric components as following

$$\frac{1}{3}\delta^{ab}_{ij}\Delta_1 + \delta^{ab}_{ji}\Delta_8 - \frac{1}{3}\delta^{ab}_{ij}\Delta_8 = (\delta^{ab}_{ij}+\delta^{ab}_{ji})\Delta_S + (\delta^{ab}_{ij}-\delta^{ab}_{ji})\Delta_A; \tag{B1}$$

with definition:

$$\Delta_A = \frac{1}{6}\Delta_1 - \frac{2}{3}\Delta_8; \qquad \Delta_S = \frac{1}{6}\Delta_1 + \frac{1}{3}\Delta_8. \tag{B2}$$

In the case of finite strange quark mass, we have two anti-symmetric components and three symmetric components. We can extract these components as following. For (u;d) anti-symmetric part ((u;d) − (d;u)), we have

$$\Delta_A^{ud} = -\frac{3}{4}\Delta_{83} + \frac{1}{12}\Delta_{81} + \frac{\sqrt{2}}{6}\Delta_{\Delta} + \frac{1}{6}\Delta_{11}. \tag{B3}$$

For (u;d) symmetric part ((u;d) + (d;u)),

$$\Delta_S^{ud} = \frac{1}{4}\Delta_{83} + \frac{1}{12}\Delta_{81} + \frac{\sqrt{2}}{6}\Delta_{\Delta} + \frac{1}{6}\Delta_{11}. \tag{B4}$$

For (u;s) or equivalently (d;s) part, we obtain

$$\Delta_A^{us(ds)} = -\frac{1}{2}\Delta_{82} - \frac{1}{6}\Delta_{81} - \frac{\sqrt{2}}{12}\Delta_{\Delta} + \frac{1}{6}\Delta_{11}; \tag{B5}$$

$$\Delta_S^{us(ds)} = +\frac{1}{2}\Delta_{82} - \frac{1}{6}\Delta_{81} - \frac{\sqrt{2}}{12}\Delta_{\Delta} + \frac{1}{6}\Delta_{11}: \tag{B6}$$

For the symmetric 2(u;u) = 2(d;d) sectors,

$$\Delta_S^{uu(dd)} = \frac{1}{4}\Delta_{83} + \frac{1}{12}\Delta_{81} + \frac{\sqrt{2}}{6}\Delta_{\Delta} + \frac{1}{6}\Delta_{11} - \Delta_S^{ud}; \tag{B7}$$

which is completely equal to $^{ud}_{S}$ by the remaining $SU(2)_V$ isospin symmetry. Finally, for $2(s;s)$ sector, we have

$$^{ss}_{S} = \frac{1}{3}\ _{81} \quad \frac{\sqrt{2}}{3} + \frac{1}{6}\ _{11}: \tag{B8}$$

If we forbid the condensation in the color-flavor symmetric channel, the three independent constraints $^{uu(dd)}_{S} = {}^{ss}_{S} = {}^{us(ds)}_{S} = 0$ are to be postulated. These give

$$_{81} = \frac{1}{3}\ _{83} + \frac{4}{3}\ _{82}; \quad = \frac{\sqrt{2}}{3}\ _{83} + \frac{\sqrt{2}}{3}\ _{82}; \quad _{11} = \frac{2}{3}\ _{83} \quad \frac{4}{3}\ _{82}: \tag{B9}$$

And the relation $^{ud}_{A} = \ _{83}; \ ^{us}_{A} = \ _{82}$ hold. The quadratic terms in the effective potential, namely the mean field potential in the effective potential can be significantly simplified in terms of $_A$ and $_S$. We saw above the linear relation

$$\begin{pmatrix} ^{ud}_{A} \\ ^{us(ud)}_{A} \\ ^{ud}_{S} \\ ^{us(ds)}_{S} \\ ^{ss}_{S} \end{pmatrix} = \begin{pmatrix} 3=4 & 0 & 1=12 & \sqrt{2}=6 & 1=6 \\ 0 & 1=2 & 1=6 & \sqrt{2}=12 & 1=6 \\ 1=4 & 0 & 1=12 & \sqrt{2}=6 & 1=6 \\ 0 & 1=2 & 1=6 & \sqrt{2}=12 & 1=6 \\ 0 & 0 & 1=3 & \sqrt{2}=3 & 1=6 \end{pmatrix} \begin{pmatrix} 1 \\ 0 \\ _{83} \\ _{82} \\ _{81} \\ _{11} \end{pmatrix}: \tag{B10}$$

In this base, the first term in Eq. (31), which is quadratic in the gap parameter, can be diagonalized as

$$\frac{3}{4g^2}(\tilde{\ }; \hat{B}\hat{A}\tilde{\ }) = \frac{12}{g^2}\ ^{ud2}_{A} + 2\ ^{us2}_{A} \quad 2\ ^{ss2}_{S} \quad 6\ ^{ud2}_{S} \quad 4\ ^{us2}_{S}: \tag{B11}$$

Note that the quadratic form is not positive definite. There are three directions in which the effective potential is unstable, corresponding to the color-flavor symmetric channels.

In general, it is hard to evaluate analytically the gap-integral of singlet mixing sector in the formula of the effective potential, Eq. (31). However, as noted in the Sec. IIB, there are two special cases in which we can calculate the gap-integral.

The pure CFL state with $M_s = 0$. This corresponds to the following off-diagonal self-energy Eq. (3). In this case, the effective potential at finite temperature reads

$$[\ _1; \ _8; \ ;T] = \frac{3}{g^2}\ _1(\ _1 + 8\ _8) \quad 8E_{cond.}(\ _8; \ ;T) \quad E_{cond.}(\ _1; \ ;T); \tag{B12}$$

with the definition

$$E_{cond.}(\ ; \ ;T) = +2 \int \frac{dq}{(2\ )^3} \log \left[\frac{\cosh\left(\sqrt{(q \quad)^2 + \ ^2}=2T\right)}{\cosh(|q \quad |=2T)} \right] + (\ \$ \ ): \tag{B13}$$

Note that the quadratic term, namely the mean field potential, can be written in the diagonal form as

$$\frac{3}{g^2}\ _1(\ _1 + 8\ _8) = \frac{36}{g^2}(\ ^2_A \quad 4\ ^2_S); \tag{B14}$$

where $_S$ and $_A$ are the symmetric and anti-symmetric component of the gap matrix Eq. (B2). The negative sign in front of ^2_S implies that the effective potential is unbound in the direction of the repulsive channels.

The 2SC state for an arbitrary value of M_s. In the case of the 2SC defined by Eq. (4), the effective potential at finite temperature becomes

$$[\ _{2SC}; \ ;T;M_s] = \frac{12}{g^2}\ ^2_{2SC} \quad 4E_{cond.}(\ _{2SC}; \ ;T): \tag{B15}$$

Note that the strange quark mass M_s does not enters this expression.

---

[1] D. Bailin and A. Love, Phys. Rep. 107, 325 (1984),

[2] M. Iwasaki and T. Iwado, Phys. Lett. B 350, 163 (1995); M. G. Alford, K. Rajagopal and F. Wilczek, Phys. Lett. B 422, 247 (1998); R. Rapp, T. Schafer, E. V. Shuryak and M. Velkovsky, Phys. Rev. Lett. 81, 53 (1998).
[3] For reviews, see K. Rajagopal and F. Wilczek, arXiv:hep-ph/0011333; M. G. Alford, Ann. Rev. Nucl. Part. Sci. 51, 131 (2001); T. Schafer, arXiv:hep-ph/0304281; D. H. Rischke, arXiv:nucl-th/0305030.
[4] M. G. Alford, K. Rajagopal and F. Wilczek, Nucl. Phys. B 537, 443 (1999).
[5] E. Shuster and D. T. Son, Nucl. Phys. B 573, 434 (2000); B. Park, M. Rho, A. Wirzba and I. Zahed, Phys. Rev. D 62, 034015 (2000).
[6] T. Schafer, Nucl. Phys. B 575, 269 (2000).
[7] N. Evans, J. Hormuzdiar, S. D. H. Hsu and M. Schwetz, Nucl. Phys. B 581, 391 (2000).
[8] S. D. H. Hsu, F. Sannino and M. Schwetz, Mod. Phys. Lett. A 16 1871 (2001).
[9] D-K. Hong and S. D. H. Hsu, Phys. Rev. D 66, 071501 (2002); D-K. Hong and S. D. H. Hsu, Phys. Rev. D 68, 034011 (2003).
[10] T. Schafer and F. Wilczek, Phys. Rev. D 60, 074014 (1999).
[11] M. Alford, J. Berges and K. Rajagopal, Nucl. Phys. B 558, 219 (1999).
[12] A. I. Larkin and Yu. N. Ovchinnikov, Zh. Eksp. Teor. Fiz. 47, 1136 (1964) [Sov. Phys. JETP 20, 762 (1965)]; P. Fulde and R. A. Ferrell, Phys. Rev. 135, A550 (1964);
[13] M. G. Alford, J. A. Bowers and K. Rajagopal, Phys. Rev. D 63, 074016 (2001); J. A. Bowers, J. Kundu, K. Rajagopal and E. Shuster, Phys. Rev. D 64, 014024 (2001); J. Kundu and K. Rajagopal, Phys. Rev. D 65, 094022 (2002); J. A. Bowers and K. Rajagopal, Phys. Rev. D 66, 065022 (2002); R. Casalbuoni and G. Nardulli, arXiv:hep-ph/0305069.
[14] T. Schafer, Phys. Rev. Lett. 85, 5531 (2000); D. B. Kaplan and S. Reddy, Phys. Rev. D 65, 054042 (2002).
[15] I. Shovkovy and M. Huang, Phys. Lett. B 564, 205 (2003); M. Huang and I. Shovkovy, arXiv:hep-ph/0307273.
[16] E. Gubankova, W. V. Liu and F. Wilczek, Phys. Rev. Lett. 91, 032001 (2003); M. Alford, C. Kouvaris and K. Rajagopal, arXiv:hep-ph/0311286.
[17] K. Iida, T. Matsuura, M. Tachibana and T. Hatsuda, arXiv:hep-ph/0312363.
[18] T. Schafer, Nucl. Phys. B 575, 269 (2000).
[19] H. Abuki, Prog. Theor. Phys. 110, 937 (2003).
[20] I. A. Shovkovy and L. C. R. Wijewardhana, Phys. Lett. B 470, 189 (1999).
[21] R. Casalbuoni, R. Gatto, G. Nardulli and M. Ruggieri, Phys. Rev. D 68, 034024 (2003).
[22] A. J. Leggett, in Modern Trends in the Theory of Condensed Matter (Springer, Berlin, 1980), p. 13; J. Phys. (Paris) 41, C7-19 (1980).
[23] P. Nozieres and S. Schmitt-Rink, J. Low Temp. Phys. 59, 195 (1985).
[24] U. Lombardo, P. Nozieres, P. Schuck, H. J. Schulze and A. Sedrakian, Phys. Rev. C 64, 064314 (2001).
[25] E. Babaev, Int. J. Mod. Phys. A 16, 1175 (2001).
[26] M. Matsuzaki, Phys. Rev. D 62, 017501 (2000); H. Abuki, T. Hatsuda and K. Itakura, Phys. Rev. D 65, 074014 (2002).
[27] Y. Nishida, K. Fukushima and T. Hatsuda, arXiv:hep-ph/0306066.
[28] M. Kitazawa, T. Koide, T. Kunihiro and Y. Nemoto, Phys. Rev. D 65, 091504, (2002).
[29] M. Kitazawa, T. Koide, T. Kunihiro and Y. Nemoto, arXiv:hep-ph/0309026; A. Schnell, G. Ropke and P. Schuck, Phys. Rev. Lett. 83, 1926 (1999).
[30] S. P. Klevansky, Rev. Mod. Phys. 64, 649 (1992); T. Hatsuda and T. Kunihiro, Phys. Rep. 247, 221 (1994).
[31] T. Schafer and E. Shuryak, Rev. Mod. Phys. 70, 323 (1998).
[32] T. Schafer, Phys. Rev. D 62, 094007 (2000).
[33] M. Buballa and M. Oertel, Nucl. Phys. A 703, 770 (2002).
[34] M. Buballa, arXiv:hep-ph/0402234.
[35] M. Oertel and M. Buballa, arXiv:hep-ph/0202098.
[36] M. Alford and K. Rajagopal, JHEP 0206, 031 (2002); A. W. Steiner, S. Reddy and M. Prakash, Phys. Rev. D 66, 094007 (2002); F. Neumann, M. Buballa and M. Oertel, Nucl. Phys. A 714, 481 (2003).
[37] K. Iida and G. Baym, Phys. Rev. D 63, 074018 (2001).